Characterising hardening on annealing of cold rolled aluminium AA3103 strips

Nagaraj Vinayagam Govindaraj[a], Ruben Bjørge[b], Bjørn Holmedal[a]
[a] Department of Materials Science & Engineering
[b] Department of Physics
Norwegian University of Science & Technology
7491, Trondheim
Norway

Corresponding author:
Nagaraj Vinayagam Govindaraj
Department of Materials Science and Engineering
Norwegian University of Science and Technology
7491, Trondheim
Norway
Phone: +47 735 96785
Fax: +47 735 50203
e-mail: nagaraj.vinayagam@material.ntnu.no

Abstract

AA3103 aluminium strips were cold rolled to various von Mises strains up to 4.7. In addition, two severely deformed conditions were obtained by one and four cycles of cold accumulated roll bonding subsequent to cold rolling to a strain of 4.2. For cases of subsequent annealing at 225ºC for 10 minutes, an increase in the ultimate tensile strength was observed at the rolling strains of 1.7 and above. Similar hardening is observed for a wide range of temperature-time combinations for temperatures above 150ºC. The yield stress is also increased with further cold rolling by a few per cent. The magnitude of the increase in strength on annealing increased with increasing strain. Electron backscatter diffraction and transmission electron microscopy studies showed no significant changes in the high or low angle grain boundary spacing by this annealing. A systematic investigation on the role played by Si and Mn was made by different homogenization treatments of AA3103 and of an AlSi alloy. Based on tensile tests, differential scanning calorimetry and electrical conductivity measurements it is concluded that Mn plays a major role. The exact mechanisms causing hardening on annealing are not identified, but by elimination of other explanations it is suggested that some clustering or precipitation mechanism is involved.

Keywords: hardening on annealing, aluminium alloys, clustering, precipitation

1. Introduction

AA3103 aluminium alloy belongs to the group of non-heat treatable aluminium alloys where the strength is obtained mainly by cold rolling (CR). Some additional strength can be obtained from the alloying elements Mn and Si either present in solid solution [1] or forming dispersoids during homogenization treatment, subsequent warm rolling and annealing process steps. In heat exchanger applications, every strength contribution including hardening on annealing (HOA) is valuable since the use of stronger alloys is limited by brazeability requirements and additions of Mn decrease the thermal conductivity.

A conventional annealing treatment would reduce the strength and increase the ductility. However, in sharp contrast to the conventional property changes associated with annealing, it has been reported that commercial purity Al subjected to accumulated roll bonding (ARB) exhibits an increase in strength and a loss of ductility after a low temperature annealing treatment [2]. This was reported to be the HOA behaviour exhibited by nanostructured materials [3]. In the current paper a similar phenomenon is investigated for an AA3103 alloy, not only in the severely deformed condition but also in the cold rolled condition that is not nanostructured.

The HOA behaviour in commercial pure nanostructured Al was attributed to the limitation of dislocation sources [3]. It is recognised in the tensile curves as a yield point. A 15% thickness reduction by cold rolling subsequent to the annealing approximately restores the as-deformed behaviour [3]. This phenomenon has been observed in interstitial free steels, nickel and aluminium alloys of different purity levels [4] and it is generally obtained by a low temperature annealing treatment subsequent to severe plastic deformation by ARB. However, the full range of metals and alloys exhibiting this phenomenon has not yet been explored.

Investigations of HOA so far have mainly considered severe plastic deformation obtained by ARB, equal channel angular pressing and heavy cold rolling [5]. However, since the HOA mechanism is obtained for ARB of high purity aluminium with grain sizes at least a few micrometers [6], our attention should not be limited only to the nanostructured materials. Most investigations of HOA have considered low temperature annealing, where the temperature that gives the peak hardness after about half an hour is applied. This is the practical limit for the time required in air furnace annealing. At longer holding times the

competing mechanism of softening by static recovery of the dislocation structures will soften the material. However, it is interesting to consider higher temperatures and lower holding times to investigate if the peak hardness can be optimized. Experimentally this can be done in salt baths in the laboratory or by electric pulse annealing. Surprisingly, the electric pulse annealing of commercially pure aluminium somehow seems to enhance the HOA and a significantly higher peak stress can be obtained at similar or lower temperatures during a few minutes of pulsing [5].

HOA behaviour is observed in this work in AA3103 alloy, where Mn is the main alloying element present in solid solution and as part of particles together with Fe and Si. It is interesting to note that a similar phenomenon of HOA is reported in a recent work by Lee et al. [7] for commercially pure aluminium with various Mn additions, but with main focus on annealing at higher temperatures and longer holding times. They suggest that precipitation of Si is responsible for the observed HOA in their case. However, such precipitates would be very small in size after the low temperature annealing and can be a challenge to be observed in the microstructure for a verification of this assumption.

Precipitation of Si prior to recrystallization has also been reported earlier in a cold rolled Al-Fe-Si alloy during annealing over a broad range of temperatures and times [8]. The cold rolling before the annealing treatment enhances the Si precipitation. It is a possibility that precipitation of Si can occur during low temperature annealing and could contribute to HOA. However, the HOA behaviour reported in the current paper is at even shorter annealing times and smaller strains and only partly overlapping the lower temperature-time range in the investigation by Lee et al. [7]. Interestingly, commercially pure aluminium qualities commonly contain similar amounts of Si as in AA3103 and a HOA mechanism caused by Si would be the case for AA1XXX series alloys as well.

In this paper HOA behaviour in the AA3103 alloy is investigated. Tensile tests are used to quantify its extent. A wide range of combinations of temperatures and annealing times are investigated for various strain levels to give an overview of the HOA behaviour in the alloy considered. The probability of different factors like dislocation source limitation, low angle grain boundaries (LAGB), texture changes and clustering of alloying elements or precipitation contributing to HOA is examined. The amounts of Mn and Si in solid solution are varied by

different homogenization treatments on the AA3103 alloy and by investigation of an additional Al-Si alloy, and the impact of these elements on the extent of HOA are discussed.

2. Experimental methodology

The materials used in this study were an AA3103 alloy and an AlSi alloy with chemical compositions given in Table 1. Billets in the as-cast condition (dimension 20x200x50 mm) were first subjected to homogenization treatments as indicated in Table 2. These billets were further subjected to rolling at room temperature (20-25°C), and a series of strain levels from 0.57 to 4.7 were achieved by cold rolling to various final thicknesses down to 0.5mm in multiple pass. The average pass reduced the thickness by approximately 0.5 mm. From this batch of cold rolled material, some of the strips rolled to a strain of 4.2 were further subjected to one or four cycles of ARB. The bonding surfaces were degreased with acetone and brushed with a rotary wire brush (wire material: carbon steel, wire diameter: 0.3 mm, brush diameter: 100 mm, brush speed 3800 rpm). The two strips were then riveted at the ends to form a stack and subjected to roll bonding within 2 minutes after the surface preparation to minimise the effects of adsorbed moisture and contamination. Roll bonding was carried out in a laboratory two-high rolling mill with roll diameter of 205 mm at room temperature with a constant reduction of 50% from 1mm to 0.5 mm in each pass. All the steps from surface preparation to roll bonding constitute one cycle of ARB. After the first cycle, the samples were cut, degreased, wire brushed and then stacked for the next cycle of ARB. The width of all ARB strips was restricted to a minimum of 20 mm after trimming of edges between each pass.

Table 1. Composition of the alloys, in wt%.

Alloy\Element	Si	Mn	Fe	Al
AA3103	0.12	0.98	0.54	rest
AlSi	0.50	-	0.15	rest

Table 2. Homogenization treatments given to AA3103 and Al-Si aluminium alloys.

Alloy	Homogenization
AA3103-NH	None
AA3103-1	Heating to 610°C at the rate of 150 °C/hour, holding for 4 hours followed by water quenching.
AA3103-2	Heating to 600°C at the rate of 50 °C/hour , holding for 4 hours, controlled cooling to 500°C at the rate of 25°C/hour, holding for 4 hours followed by water quenching.
AlSi-1	Heating to 560°C at the rate of 100°C/hour, holding for 6 hours followed by water quenching.
AlSi-2	Heating to 560°C at the rate of 100°C/hour, holding for 6 hours, and controlled cooling to 350°C at the rate of 20°C/hour followed by water quenching.

The annealing treatments were done in a Nabertherm air convection furnace, at which the specimens were held for the respective times and then quenched in water to room temperature.

Samples for the tensile test were machined out along the rolling direction (RD) of the strips in the as-deformed and annealed condition according to the ASTM standard E8M. Tensile tests were performed at a crosshead speed of 2 mm/min in an MTS 810 tensile testing machine.

Electrical conductivity measurements were performed on the cold rolled samples in the as-deformed and annealed conditions to distinguish the amount of Mn in solid solution. A Foerster Sigmatest sigmascope was used for the measurements.

Microstructures of the samples deformed to low strains were characterized in the as-deformed and annealed conditions using electron backscatter diffraction (EBSD) data obtained from a Zeiss Ultra FEGSEM equipped with a NORDIF UF1000 detector and analysed using TSL OIM 6.0 software. Misorientation across the sub-grain boundaries was also evaluated for some strain levels in the as-deformed and annealed condition. EBSD scans were performed in the rolling direction and normal direction plane at the centre of the thickness.

Microstructure of selected severely deformed samples in the as-deformed and annealed conditions was characterized by transmission electron microscopy (TEM). Thin foils were prepared from the strips by twin jet electro polishing in a solution of 33.3% nitric acid in

methanol at -25°C. The foils were examined on a Philips CM30 microscope with a LaB_6 filament at 150 kV with the beam along the normal direction.

Texture measurements were carried out on representative samples at specific strain levels from the cold rolled and ARB material in both the as-deformed and annealed conditions. The measurements were performed on a Siemens D5000 texture goniometer.

Differential Scanning Calorimetry (DSC) scans were performed on the cold rolled and on the severely deformed samples in the as-deformed and annealed conditions to observe changes in enthalpy associated with precipitation and softening events. Scans were run on a Sensys DSC setup from 30ºC to 550ºC at a heating rate of 10ºC/min in helium atmosphere. The scans were analysed for peaks characteristic of precipitation during annealing.

3. Results

3.1 Changes in mechanical properties on annealing AA3103-1 deformed to different strains at various temperature-time combinations

Annealing trials on the samples cold rolled to the range of von Mises strains from 1.15 to 4.7 were first carried out extensively at various combinations of temperature and time for AA3103-1, the homogenisation treatment corresponding to a typical industrial homogenisation cycle. Examples of engineering stress-strain curves of AA3103-1 are presented in Figure 1 for a range of von Mises strains of the sheet in the as-deformed condition and compared to similar curves with a subsequent low-temperature annealing at 225°C for 10 minutes. The purpose of this figure is to show the differences between annealed and as deformed conditions. It is to be noted that a comparison of the post uniform elongation between tensile tests from sheets at different strains is not possible, except for between the largest rolling strain (CR 4.2) and the two ARB samples, for which the tensile samples were cut from sheets of similar thicknesses. In the samples deformed to a strain of 1.15 the annealing treatment increases the tensile elongation without causing a significant change in the tensile strength. A small drop in the yield strength can be observed in this case. At the strain of 1.7 the tensile elongation of the annealed sample is almost the same as for the as-rolled strip and the tensile strength is only slightly higher. Further, at the strain of 2.3, the tensile elongation is decreased and the ultimate tensile strength (UTS) slightly increased after

the annealing. This trend of increased tensile strength and decreased elongation on annealing is similar for CR 4.2 and the two severely deformed samples, achieved partly by ARB.

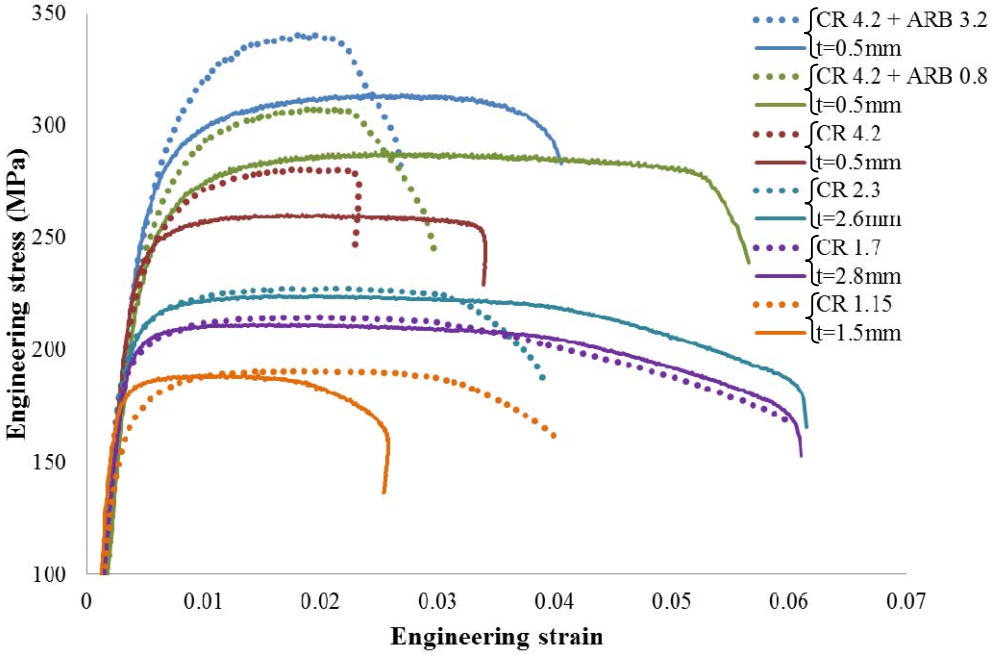

Figure 1. Engineering stress-strain curves of AA3103-1 strips at different strain levels in the as-deformed and annealed conditions represented by solid lines and dotted lines respectively - annealing at 225°C in 10 minutes. Note that the thicknesses of the tensile specimens are different at various strains, as indicated by 't' in the figure.

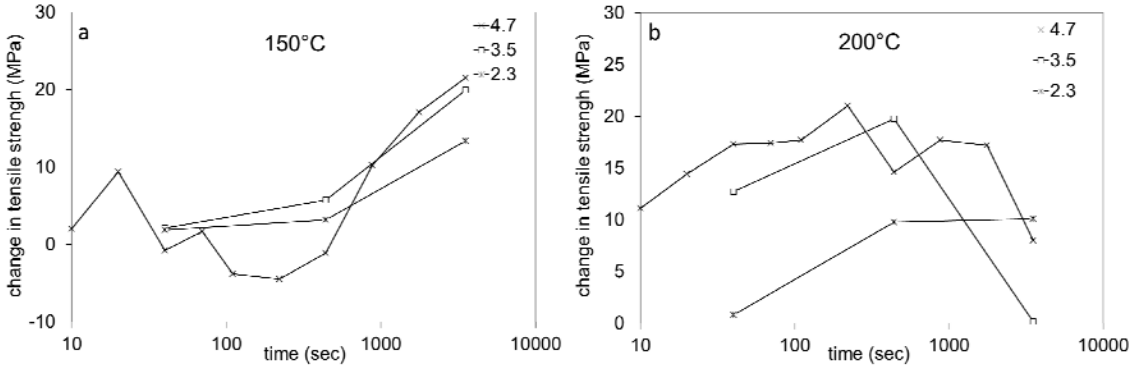

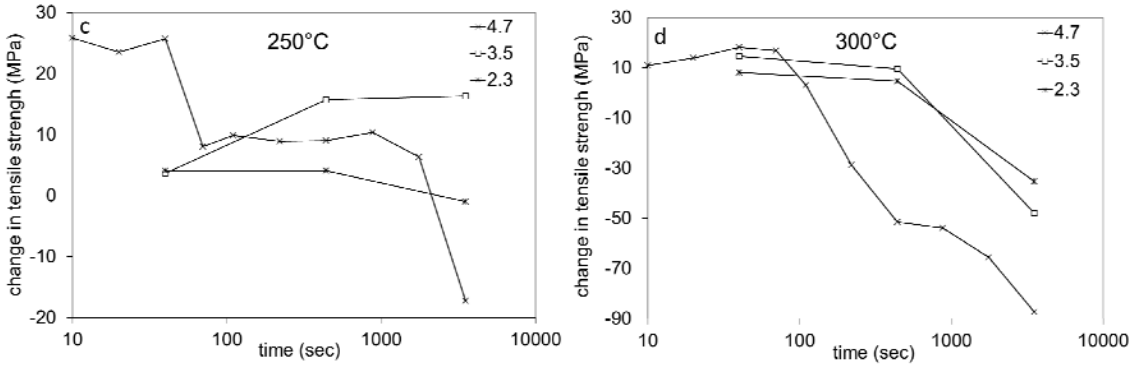

Figure 2. Changes in the tensile strength of AA3103-1 due to hardening on annealing over temperatures a) 150 b) 200 c) 250 and d) 300°C as a function of time for rolling strains 2.3, 3.5 and 4.7.

The optimum temperature - time window for maximum hardening was identified by carrying out a series of annealing trials on the AA3103-1 alloy at the strains from 2.3 to 4.7. Figure 2a-d show the change in tensile strength due to HOA over the temperatures from 150°C to 300°C and times from 40 seconds to 3520 seconds for the von Mises strain levels 2.3, 3.5 and 4.7. It is to be noted that only one tensile test was made for each point causing a considerable spread in the curves with a degree of experimental error. Nevertheless, a clear trend can be observed over increasing strain levels and temperatures and the results can be used for comparison and guidance. These plots show that with increase in strain at a given temperature, the hardening peak shifts from longer times to shorter times indicating a shift in softening kinetics. The maximum obtained increase of the hardening peak increases with increasing strain.

Annealing at 225ºC for 10 minutes was chosen as the reference annealing step, because, at this combination of temperature and time the material exhibited considerable hardening on annealing at all strains of interest, i.e. this point is situated on a quite flat region close to the peak hardening condition for the strains considered in Figure 2.

It can be seen by carefully inspection of Fig 1 that the transition from elastic loading to diffuse and localised necking is not very sharp. The increase in the yield stress as a function of the pre-strains is shown in Figure 3. It can be observed that for the annealing at 225ºC for 10 minutes a notable increase in the 0.2 % offset yield strength ($Rp_{0.2}$) cannot be observed up to a strain of 3.5. However, considerable increase can be observed in the 0.5% offset yield

strength ($R_{p0.5}$) from strains beyond 3.5. It can also be observed in figure 3 that the increase in UTS increases with increasing strain except for the two smallest strain levels of 0.57 and 1.15. Since the uniform strain is small in all these cases, the UTS can be considered to approximately correspond to R_{p1}. A 5 MPa increase in the UTS shows up at the strain level of 1.7 and with further increase in strain, the magnitude of increase in strength increases continuously with samples strained to a level of 7.4 exhibiting an increase of 30 MPa. If optimal time-temperature combinations instead of 225ºC - 10 minutes were applied for each strain level in Figure 3, the difference in the tensile strength between annealed and as-deformed conditions would probably have been slightly larger.

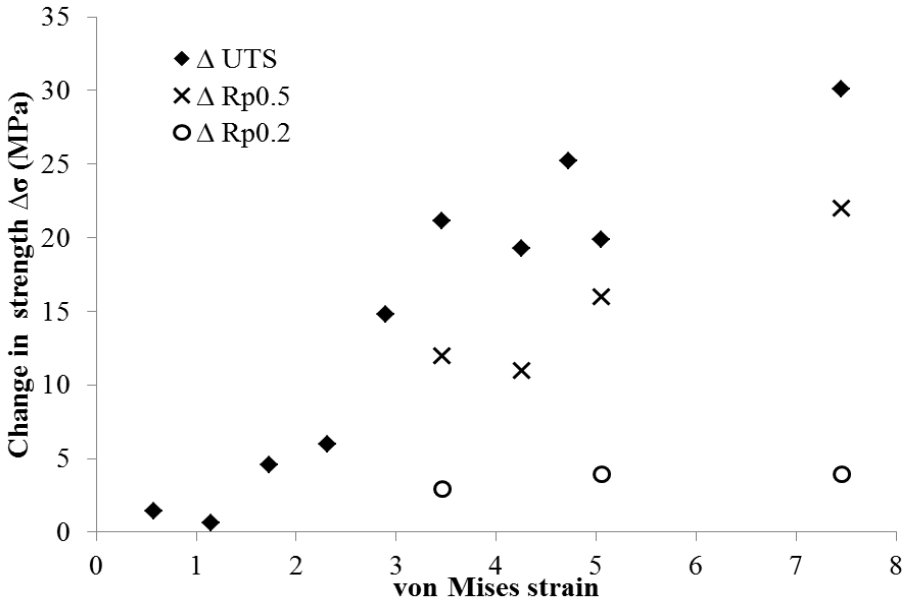

Figure 3. Magnitude of increase in strength in AA3103-1 over various strain levels on annealing at 225 °C for 10 minutes.

Figure 4 shows that the strength subsequent to an additional 15% rolling after annealing is similar to that of the annealed AA3103-1 material. Also the tensile elongation remains decreased. Visual inspection of the tensile specimens subsequent to fracture showed that the necking behaviour and the necking area was very similar for the as-rolled sample, the annealed sample and the annealed sample subjected to an additional 15% rolling before the tensile testing. Note however from Figure 4, that after the rolling the elasto-plastic transition is much sharper and a true increase in the yield stress has been achieved, i.e. the UTS subsequent to the annealing is transformed into $Rp_{0.2}$ subsequent to the 15% rolling.

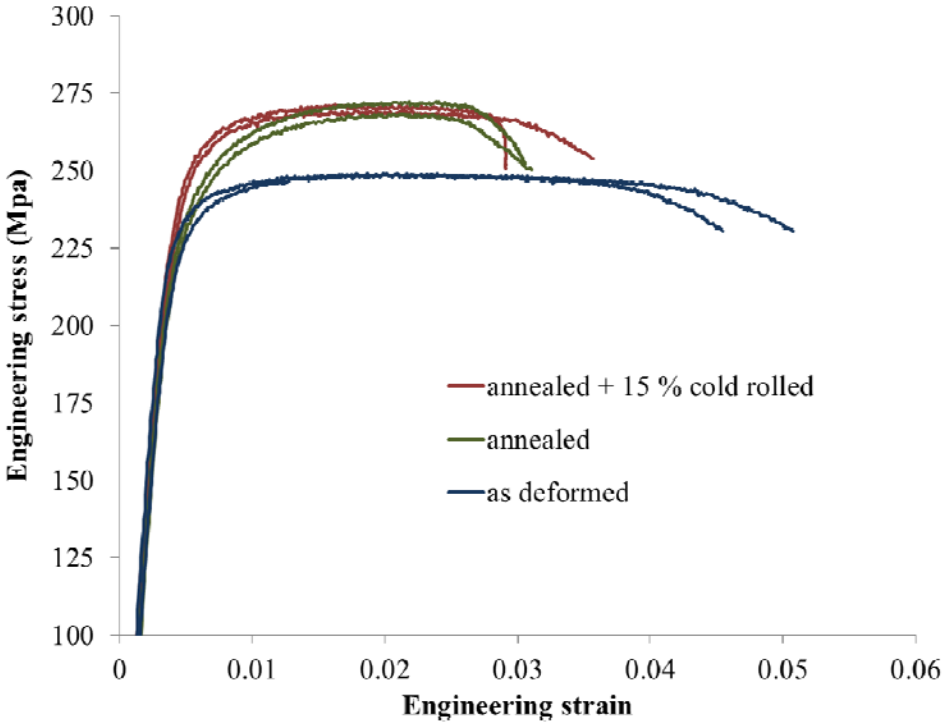

Figure 4. Engineering stress-strain curves of AA3103-1 at a rolling strain of 3.5 in the as-deformed, annealed and annealed + 15 % cold rolled conditions, two parallels are represented in each case.

Figure 5 shows how the UTS slowly decays with longer annealing times. It is to be noted that due to limited amount of material the values presented in Figure 5 are based on one tensile test for each case and hence, may include a degree of experimental scatter. Nevertheless, a clear trend can be observed, where the UTS is still above the as deformed strength after 4 hours of annealing.

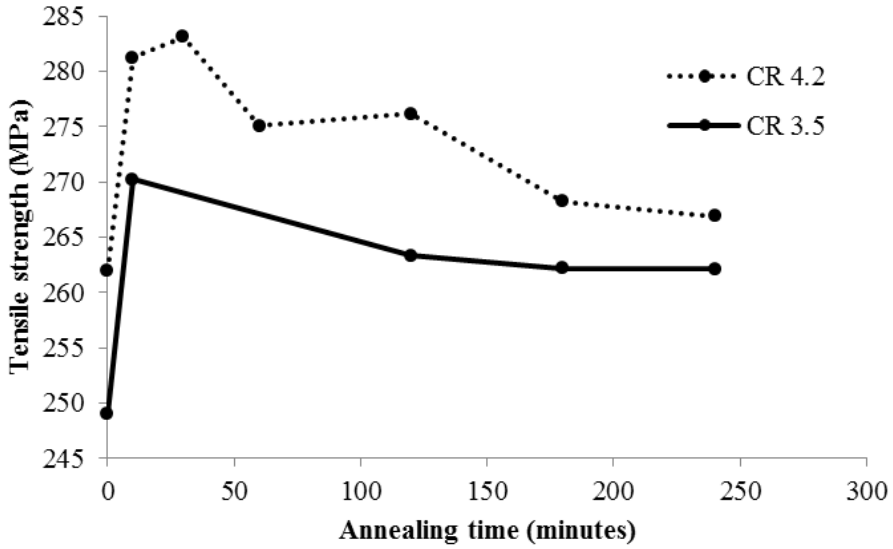

Figure 5. Change in tensile strength of AA3103-1 samples cold rolled to strains of 3.5 and 4.2 on annealing at 225°C for longer times. Annealing time '0' minutes corresponds to as-deformed samples.

3.2 Texture and substructure investigation in AA3103-1.

The AA3103 alloy used in this investigation is the same as investigated by Zhao et al. [9]. The average grain size in the as-cast condition is about 100 μm. A characterization of the decrease of subgrain size as a function of rolling strain up to a von Mises strain of 3.3, as well as constituent particles and dipsersoids, can be found in [9]. The difference between macro-texture of the deformed and annealed specimens is presented in the form of (111) pole figures in Figure 6. These pole figures show orientations that correspond to typical deformation texture in cold rolled aluminium. It can be observed that the annealing treatment at 225°C for 10 minutes causes no significant change in the macro-texture in neither the cold rolled samples at a strain of 4.2 nor the severely deformed samples at a strain of 7.4.

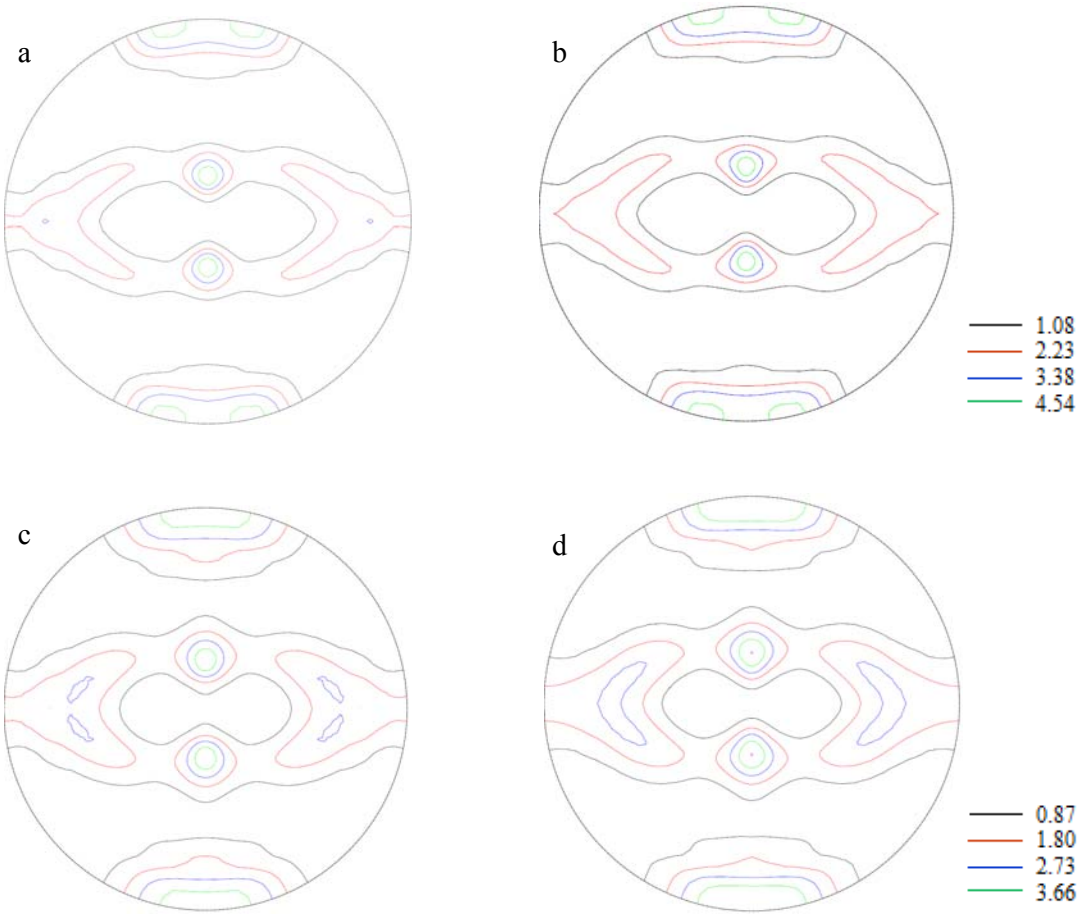

Figure 6. (111) Pole Figure s of AA3103-1 samples in different conditions a) deformed to a strain of 4.2 b) deformed to a strain of 4.2 and annealed at 225°C /10 minutes c) deformed to a strain of 7.4 d) deformed to a strain of 7.4 and annealed at 225°C /10 minutes. Iso-intensity lines for each strain level are provided on the right.

A low angle grain boundary (LAGB) map for boundaries with misorientations between 2° and 15° superimposed over the image quality map is presented in Figure 7a for the samples deformed to a von Mises strain of 2.3. In this deformed structure the subgrain boundaries are difficult to identify in the measurement. A similar map of the sample after annealing at 225°C for 10 minutes is shown in Figure 7b and reveals slightly more distinct subgrains. A number of EBSD scans were performed on different areas of the annealed material. Misorientation data for the boundaries between 2° and 15 ° presented in Figure 8 shows that there is a tendency for a very small shift towards higher misorientation angles after annealing, for which the measured average misorientation of LAGB's increases from 5.3 degrees to 5.7 degrees on annealing. However, this difference is in the same range as the experimental error. At the smaller von Mises strain of 1.15 the same annealing treatment resulted in a small

decrease in the average subgrain misorientation, from 5.2 in the as deformed condition to 4.7 after annealing. These changes are within the experimental spread and indicate that the annealing did not affect the subgrain structure notably.

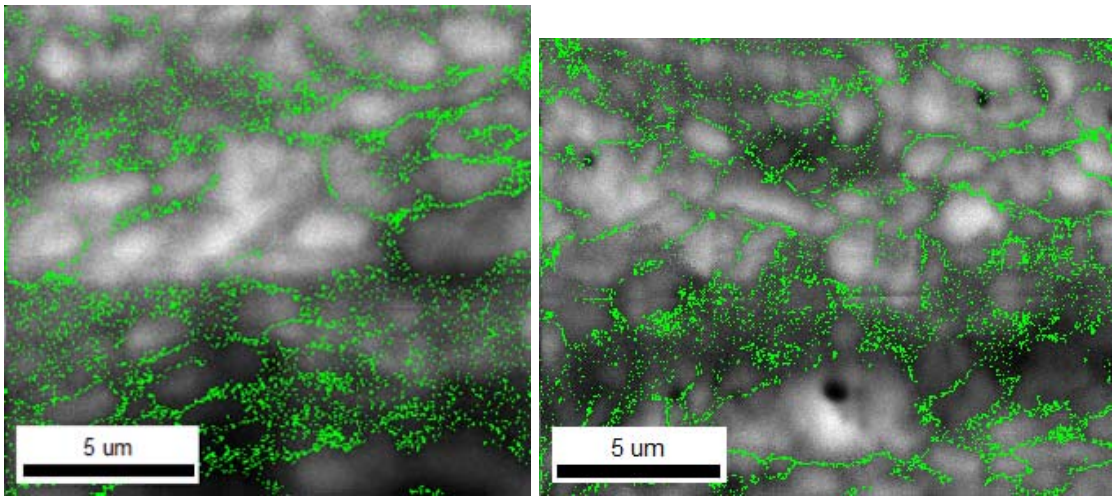

a) b)

Figure 7. Low angle grain boundary map superimposed over image quality map from EBSD for a) for the AA3103-1 alloy deformed to strain of 2.3 b) for the AA3103-1 deformed to a strain of 2.3 and annealed at 225°C for 10 minutes.

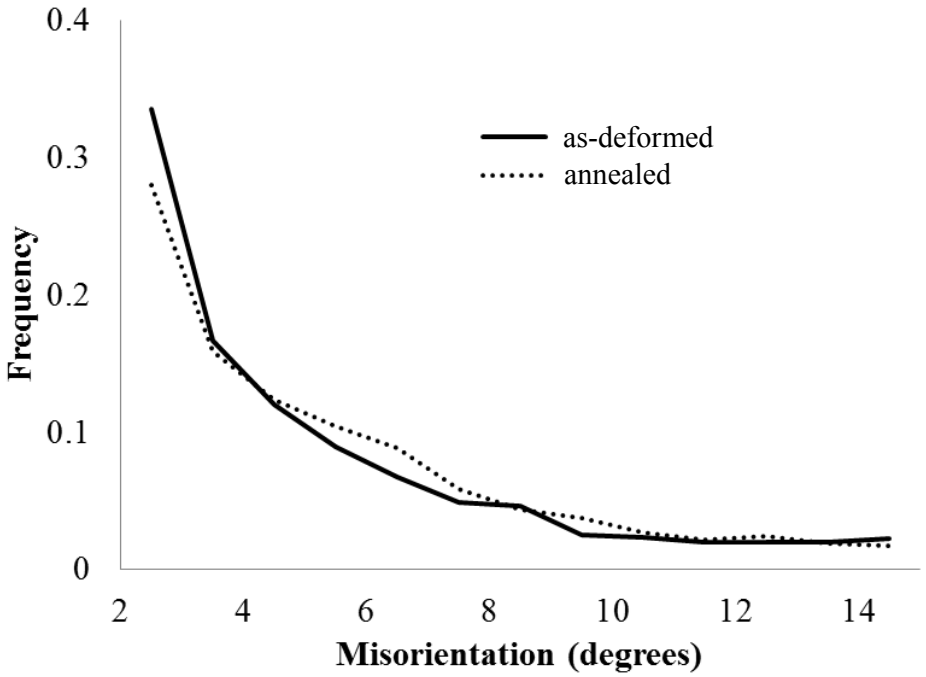

Figure 8. Comparison of misorientation across low angle grain boundaries between AA3103-1 samples deformed to a strain of 2.3 and samples further annealed at 225°C for 10 minutes after the deformation.

As EBSD became very challenging at large strains, TEM investigations were performed on some selected samples to look for microstructural changes after the short low-temperature annealing. Figure 9 shows examples of the subgrain structure before and after annealing at 225°C for 10 minutes for a sample with a von Mises strain of about 4.2. No distinct difference could be observed between the two conditions.

Attempts were made with TEM to look for precipitated particles subsequent to the annealing at 225˚C for 10 minutes for a sample deformed to a strain of 4.2. With the given resolution of the instrument no particles could be observed. Further high resolution TEM or atom probe investigations were out of the scope of this work. However, a prolonged annealing at 225°C for 4 hours instead of 10 minutes resulted in formation of small observable precipitates in the size range 10-20 nm near the sub-grain boundary in the sample, as shown in Figure 10.

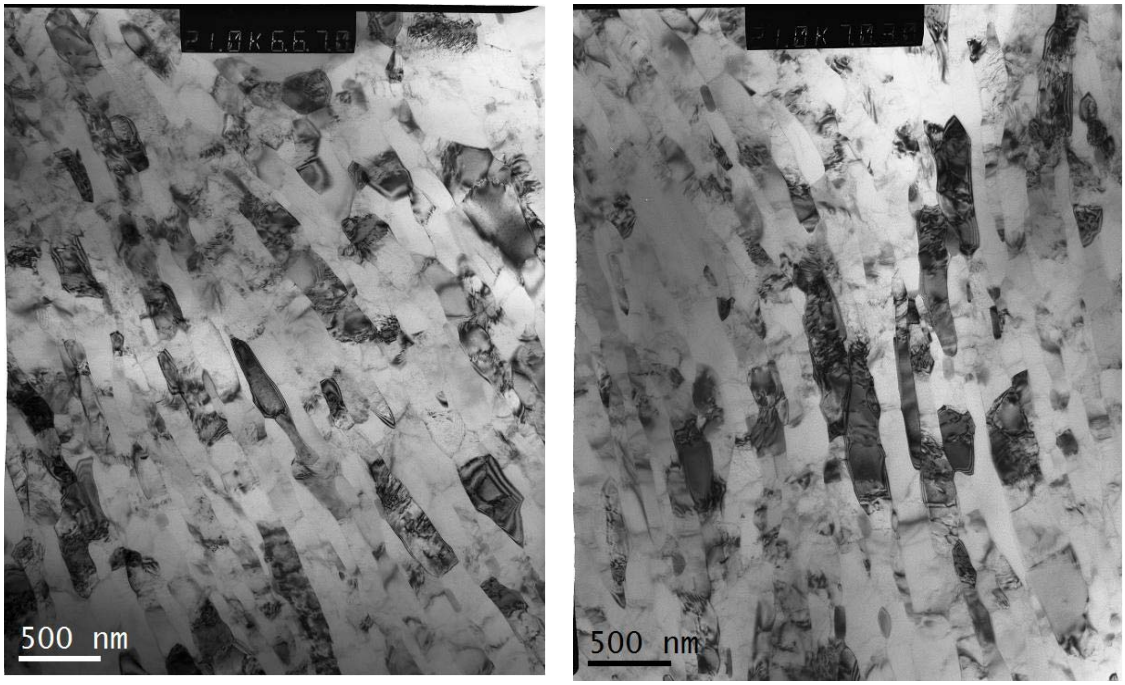

a b

Figure 9. TEM images of subgrain structure of AA3103-1 samples a) cold rolled to strains of 4.2 followed by one pass ARB. b) after further annealing at 225°C for 10 minutes. Images obtained with the beam along the transverse direction.

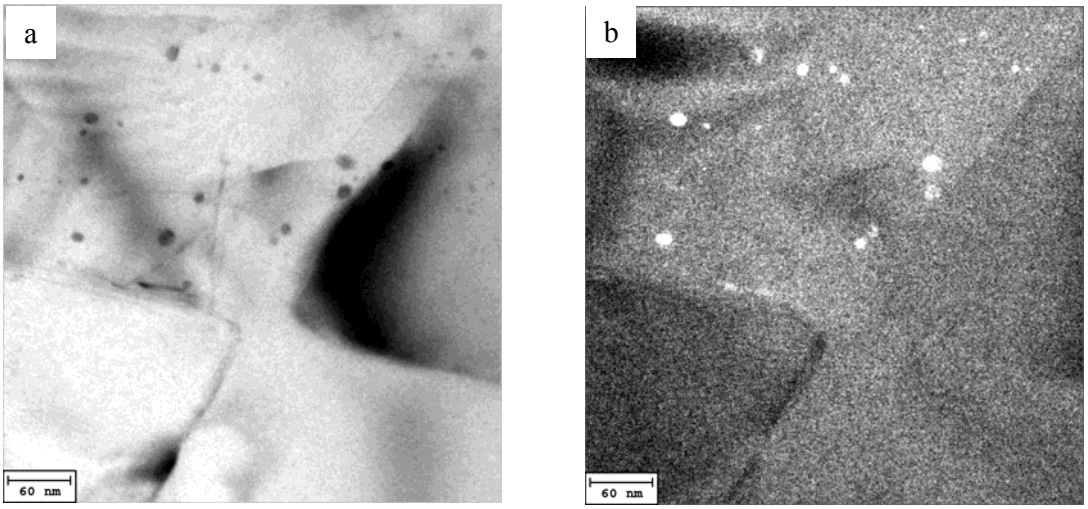

Figure 10. (a) Bright field transmission electron microscopy image and (b) corresponding dark field image showing precipitates at the sub-grain boundary in AA3103-1 samples deformed to a strain of 4.2 and annealed at 225°C for 4 hours.

3.3 Electrical conductivity changes during annealing AA3103-1 samples

The electrical conductivity is very sensitive to the content of Mn in solid solution. It can be observed in Figure 11 that the conductivity does not change much on annealing in 10 minutes of materials deformed to a range of strains. Each point corresponds to an average of 10 measurements with a small spread similar in magnitude as the difference between as-deformed and annealed cases.

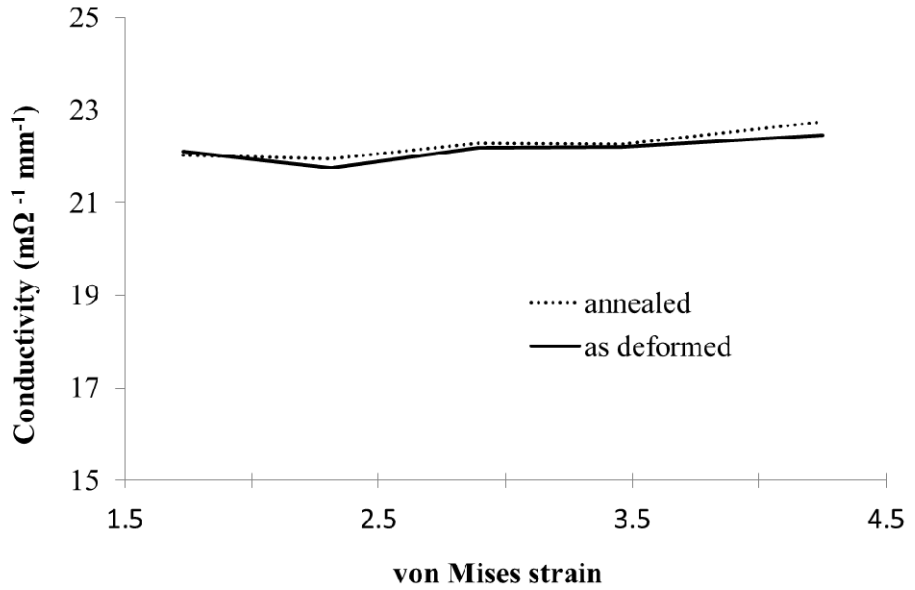

Figure 11. Conductivity changes on annealing AA 3103-1 alloy deformed to various strains at 225°C for 10 minutes.

Figure 12 shows conductivity as a function of annealing time during isothermal annealing at 225°C of the AA3103 alloy deformed to a strain of 3.5. A small increase occurs instantly during the heating, followed by a weak but continuous increase in the conductivity.

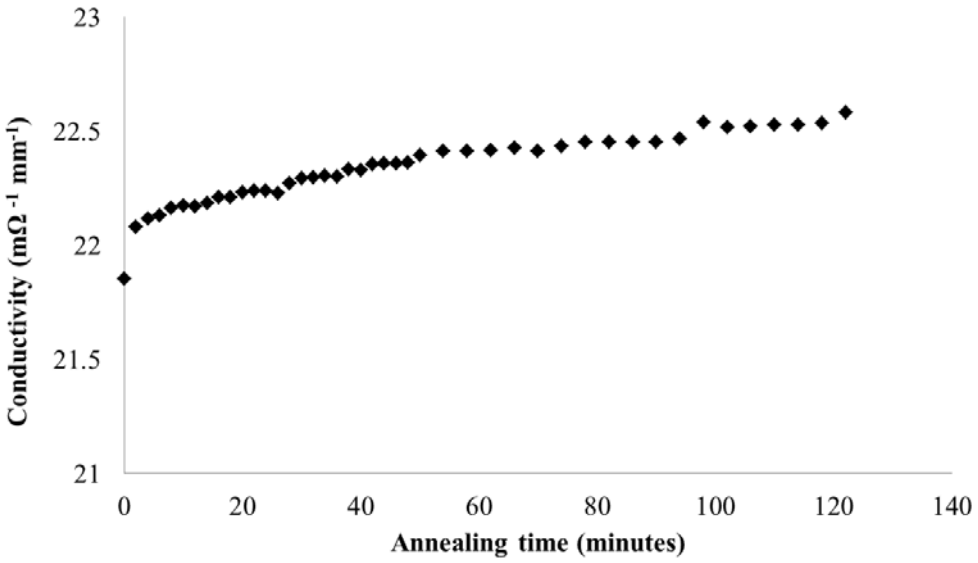

Figure 12. Detailed conductivity changes during isothermal aging at 225°C of the AA3103-1 alloy rolled to a strain of 3.5.

3.4 Differential scanning caliometry (DSC)

DSC scans were carried out at a heating rate of 10°C/min in helium atmosphere. Figure 13 compares results from DSC experiments conducted on the cold rolled AA3103 alloy at von Mises strains of 3.5, 5 and 7.4. At the lowermost strain, three exothermic peaks, occurring at about 210, 290 and 380˚C, can be identified as indicated by the arrows in the Figure 13. The peak at 290˚C is weak but well defined at the pre-strain of 3.5. A more broad peak occurs in the temperature range of interest from 200-230˚C. At the two largest strains involving ARB a strong exothermic peak appeared in the range 250-300˚C. This peak overlaps with the two lowermost peaks observed at the lower strain.

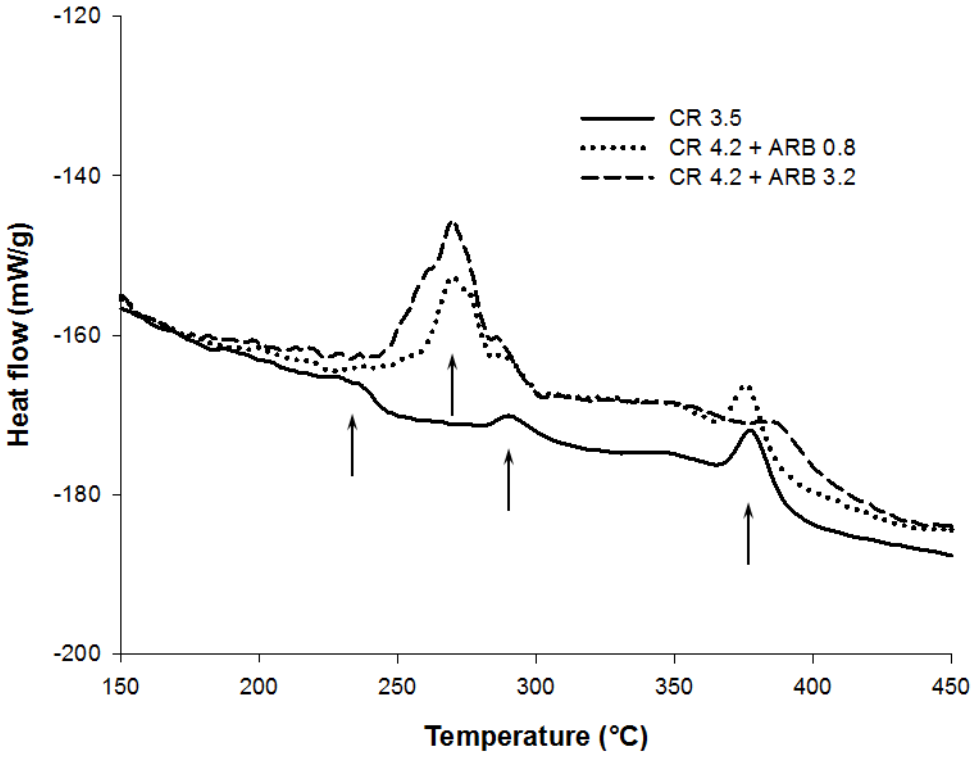

Figure 13. DSC curves of cold rolled and severely deformed AA3103-1. Arrows indicate exothermic peaks.

3.5 Effect of different homogenization treatments on AA3103 and Al-Si alloys

The major part of the experimental work is concerning the AA3103-1 condition. In order to investigate the influence of the alloying elements in solid solution, complementary experiments were performed with alloys in different conditions. AA3103 was investigated in two other conditions: - AA3103NH without homogenization and AA3103-2 with an extended homogenization. An Al-Si alloy that was similar to AA3103 but without Mn was investigated in two homogenization conditions: - AlSi-1 and AlSi-2.

One way to have more of the alloying elements in solid solution is to skip the homogenization. Figure 14 shows that the homogenization at 610°C for 4 hours results in a considerably lower strength in AA3103-1 than in the as-cast, non-homogenized AA3103NH. It is to be noted from Figure 14 that this homogenization treatment causes a change only in the tensile strengths but not in the extent of HOA. The difference between the as-deformed and annealed material is almost the same in both conditions.

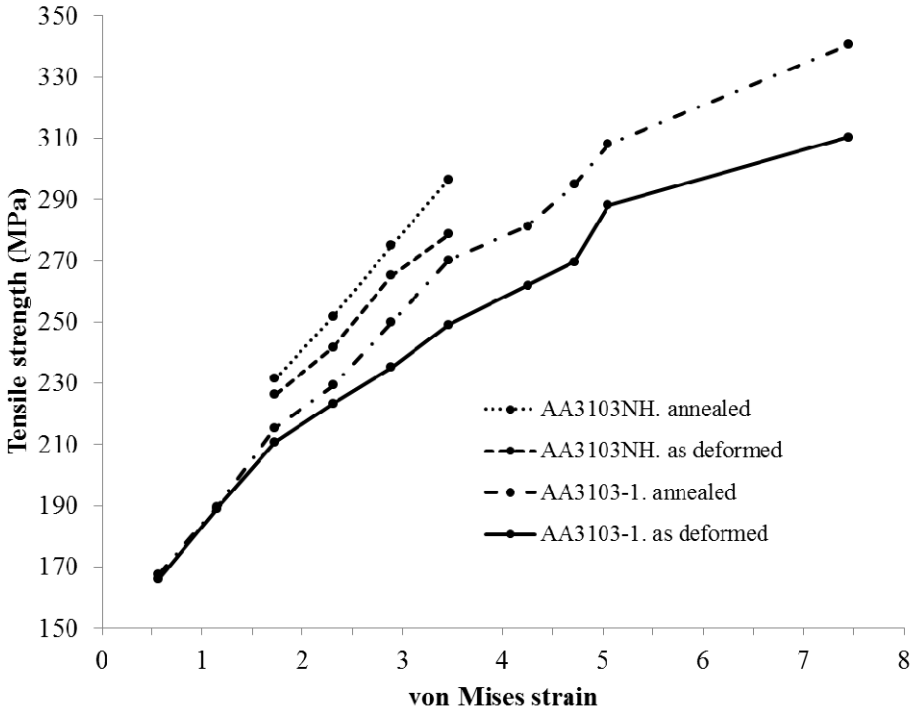

Figure 14. Effect of homogenization on the hardening on annealing behaviour of AA3103.

Figure 15 shows that the HOA behaviour is not observed at all in the Al-Si alloy for any of its two homogenizations. Also, the homogenization condition AA3103-2 that had the lowest amount of Si in solid solution exhibited a significant HOA among the three homogenization conditions of AA3103.

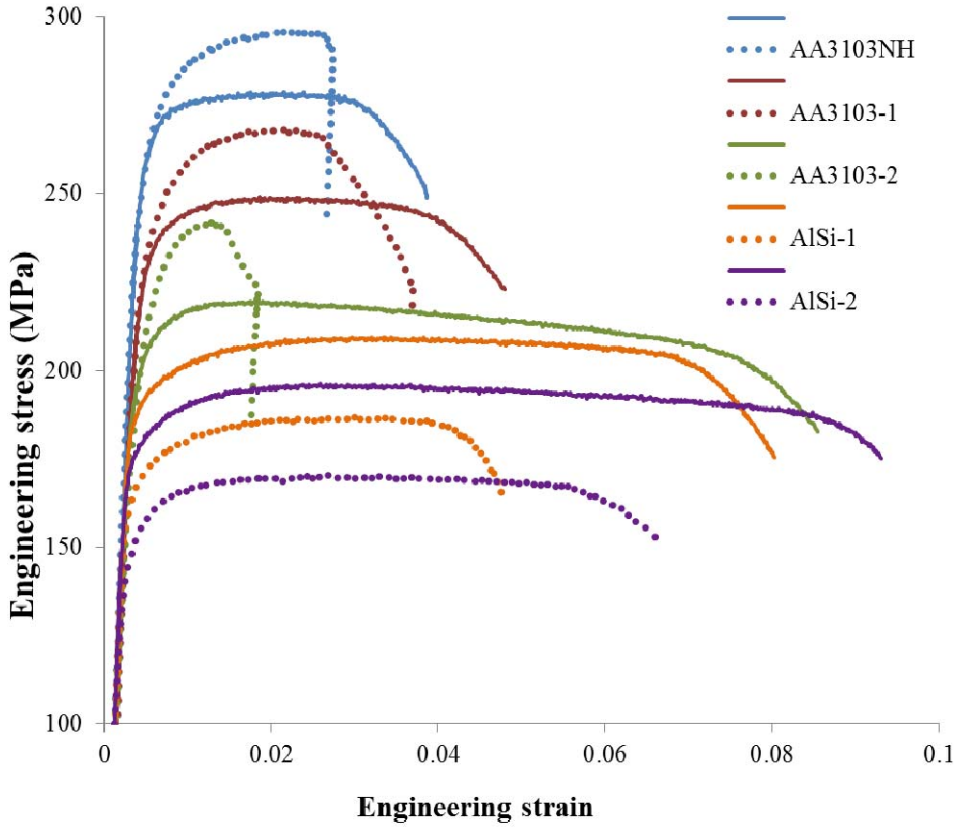

Figure 15. Engineering stress-strain curves of the AA3103 and Al-Si alloys with the different homogenizations defined in Table 2. Curves of samples as deformed (solid lines) to a strain of 3.5 are compared with those of samples further annealed at 225°C for 10 minutes (dotted lines).

4. Discussion

HOA is the phenomenon of increase in strength of a material due to annealing at low temperatures, where excessive and heterogeneous coarsening of the structure does not occur. No significant changes of the grain boundary spacing or subgrain structure can be observed from texture observations in Figure 6, EBSD results in figure 7-8 or TEM investigations in Figure 9.

HOA observed in this work is strictly obtained only at the largest strains, because the additional strength is gained through a rapid initial work hardening during about 1% strain by the tensile test subsequent to the annealing. In theory, if the material was perfectly hardened, $R_{p0.2}$ and UTS should more or less coincide in an ideal monotonic test, due to immediate necking with the low stage IV work hardening. This can be attributed to the transient

behaviour due to the necking and also that the test involves a strain path change from plane strain compression to tensile mode. The tensile tests in figure 1 reveal that there is a slight drop in the yield strength for the case of CR 1.15. Hence, there occurs a transition from softening on annealing to hardening on annealing at the specific temperature and time of 225°C and 10 minutes, in the strain range 1.15 – 1.7. Consequently, a threshold strain limit exists for exhibiting this hardening on annealing behaviour in cold rolled AA3103 alloys.

The initial work hardening of the annealed tensile samples can be analysed in terms of how it alters the balance between storage and dynamic recovery of dislocations during subsequent deformation. The very rapid initial work hardening in the tensile tests cannot be explained by changes of the storage rate of dislocations, because that would require severe slip length restrictions by introduction of a significant number of new strong observable dislocation obstacles like grain boundaries or non-shearable particles. The rapid hardening is more likely caused by reduced dynamic recovery subsequent to the annealing treatment. This requires formation of weaker obstacles that can pin dislocations. It cannot be the dislocations themselves acting as such pinning points, because the annealing reduces their amount, and rearrangements into stronger obstacles would have been erased by the further 15% rolling. Also static strain ageing would vanish during such subsequent rolling, as solutes would only temporarily arrest dislocations. The only options left are precipitation of small particles or rearrangement of solute atoms into clusters that pin the dislocations more efficiently than single atoms. This would decrease the dynamic recovery which would lead to a rapidly increasing dislocation density and a corresponding strong work hardening at small strains. The weak pinning of dislocations would at the same time increase the friction stress required to move dislocations. Unfortunately, such obstacles are very difficult to detect and verify by microscopic investigations.

Dislocation source limitation has been suggested as an explanation for HOA for materials deformed to very high strains, i.e. a reduction in density of potential dislocation sources as the dislocation network is reduced by the annealing. Instead dislocations have to be generated from sources at the grain boundaries at a higher stress [3, 10] during the subsequent deformation. Correlations have been reported between HOA and a reduction in the density of dislocations in the interior of the grain and a slight increase of the grain and sub-grain boundary spacing [3]. An associated decrease in the total tensile elongation similar to the one shown in Figure 1 has earlier been reported along with this type of HOA behaviour [3]. The

magnitude of strain that is required for HOA has been investigated in commercial purity ARB Al samples [11], for which HOA is reported to occur after 10 cycles of ARB but not at all after 6 cycles. In the investigated AA3103-1 the HOA can at least partly be qualitatively explained by lack of dislocation sources only for the samples involving severe plastic deformation, i.e. the ARB samples. However, HOA in the cold rolled AA3103-1 at the lower strain levels of 2.3 and 2.8, where the grain size is usually a few micrometers, warrants alternative mechanisms. A characteristic feature of the dislocation source limitation is that the sources are re-established by a small subsequent deformation, which consequently will erase the HOA. It has been reported that for the case of commercial purity aluminium, the HOA vanished with about 15% rolling subsequent to the annealing treatment [3]. In contrast, the results presented in Figure 4 show that the UTS subsequent to 15% rolling is similar to that of the annealed material. Hence, the HOA in AA3103 must have another explanation.

Interestingly, the post uniform tensile elongation is decreased for the annealed samples as compared to the as-deformed samples in Figure 1, and it remains decreased also for the subsequently 15% rolled samples in Figure 4. By visual inspection of the fracture areas of the samples significant degree of necking could be observed by the naked eye, i.e. a considerable ductility for all the samples after the tensile tests. Even though the post uniform part of the tensile curves looks shorter for the annealed samples in Figure 4, the observed necking geometry and necking area after testing appeared qualitatively similar for as-rolled, annealed and annealed + 15% rolled samples. The difference in the stress strain curves must be a result of differences in the plastic behaviour during the plastic instability in terms of work hardening, strain rate sensitivity or anisotropy caused by the HOA.

During low temperature annealing of AA3103, concurrent precipitation of Mn rich dispersoids sometimes starts during annealing earlier than recrystallization [12-14]. Concurrent precipitation during annealing can influence the evolution of the microstructure and mechanical properties [13,14]. However, the time-temperature-transformation curves for AA3103 alloys subjected to different heat treatments reveals that an annealing temperature of 225°C is too low for precipitation of such dispersoids to occur [14]. Fortunately, the electrical conductivity is very sensitive to the Mn content [15], and it can observed in Figure 11 that the annealing treatment at 225°C in 10 minutes does not cause a significant change the electrical conductivity. The contributions from Si in solid solution to the conductivity is very small and the amount of Fe in solution is too small to make a difference. However, contributions from

clusters or very small precipitates can in theory be comparable to contributions from Mn. Assuming that the small change is caused entirely by Mn, the amount available for contributing to hardening on annealing can be at most approximately 200 ppm, estimated by Matthiessen's rule based on increased conductivity due to the reduced amount of Mn in solution.

The content of alloying elements in solid solution in AA3103 alloys is generally reduced by the coarsening of Fe-rich constitutive particles during homogenization [14, 15]. Formation of dispersoids during heating and coarsening of particles during the homogenization treatment at 610°C deprives the matrix of most of the Si leaving behind a very small amount in solid solution. Figure 14 shows that the homogenization treatment causes a change only in the tensile strengths but not in the difference of UTS between the as-deformed and annealed material, which is almost the same for AA3103-1 and AA3103NH. This indicates that the higher levels of Si and Mn in solid solution in AA3103NH are of little importance for the HOA.

To investigate further the effect of the alloying elements on the extent of HOA AA3103-2 with a prolonged homogenization treatment was tested. The 4 hours extra holding time at 500°C results in particle coarsening and subsequently a very low level of Si, estimated to be lower than 400 ppm. Also the Mn level in solid solution is reduced as compared to AA3103-1. This condition has almost only Mn in solid solution but still exhibits a significant increase in UTS by HOA, similar in magnitude as for the AA3103-1 and AA3103NH. This shows that if Si in solid solution is involved in HOA, only a very small amount is required.

Silicon is an alloying element with significantly higher diffusivity than Mn and Fe in aluminium [16] and it has been reported that precipitation of Si may occur in commercially pure Al at temperatures well below 200°C [8]. Hence, it can potentially contribute to the HOA behaviour in AA3103. Lee et al. [7] compared HOA type of behaviour of a binary Al-0.5% Mn alloy with a commercial purity Al-0.5% Mn alloy containing 0.1% Si and could observe HOA only in the latter case. They concluded that the HOA had to be due to the Si. However, as can be seen from Figure 15, no HOA was observed for AlSi-1 and AlSi-2. It is thus evident that Si cannot cause hardening on annealing on its own. The annealing time of 10 minutes is a very short time at 225°C for the diffusion and precipitation of the leftover Si to occur. Also, if the contribution of Si precipitation were to account for 30 MPa in AA3103-2

this HOA mechanism would have to be remarkably effective with respect to the extremely small amount of Si available. Since the binary Al-Mn alloy investigated by Lee et al. [7] did not show any HOA, it can be inferred that a small amount of Si might still be important for the HOA in the AA3103 alloy. However, various amounts of Si in solution in AA3103NH, AA3103-1 and AA3103-2 do not greatly influence the magnitude of the HOA.

Clustering of solutes detected by 3D atom probe technique has been suggested to increase the strength in aluminium alloys with scandium, zirconium and hafnium [17]. Clustering of solute atoms is also reported to commonly occur during early stages of precipitation in Al-Mg-Si alloys [18]. Formation of such solute clusters has been suggested as a mechanism contributing to the hardening behaviour in AA3103 alloys [1]. Kenawy et al. [19] reported that in the case of a slightly deformed Al-Mn alloy, the formation of clusters of Mn and Fe atoms above 400˚C showed up as an increase in resistivity during isothermal annealing in competition with the decrease in resistivity due to decreased amount of Mn in solution, thereby resulting in a peak in the resistivity-time curve. The conductivity measurements in Figure 12 for AA3103-1 deformed to a strain of 3.5 at 225°C did not reveal any peak. Instead, a small but continuous increase in conductivity, characteristic of vacancy migration to sinks, annihilation and recovery as suggested by Kenawy et al. [19], was observed. The small increase occurring instantly during the heating is commonly observed for deformed materials and is believed to be related to the most easily annealed dislocations. Even though conductivity changes characteristic of cluster formation cannot be identified from the curve, a continuous formation of small clusters that are relatively stable at this low temperature cannot be excluded. The contribution of such clusters to electrical conductivity depends to a great extent on their size and the size of the clusters is in turn dependent on kinetics [20]. Considering the low temperatures and short times used for annealing in this work, it is likely that if clusters are formed in this case, they are so small that their contributions to electrical conductivity can hardly be distinguished from that of the solute atoms. Moreover, the temperatures involved in this work are quite low to facilitate diffusion of Mn and Fe, even along dislocation pipes, and this further strengthens the argument against diffusion of Mn and Fe to form clusters, especially in the structures without ultrafine grains. Pipe diffusion is enhanced with increased strain consistent with the increased amount of HOA.

Precipitation results in exothermic peaks in DSC. The exothermic peak occurring at about 380˚C for the lowermost strain in the DSC in Figure 13 corresponds to precipitation of the α-

Al(Mn,Fe)Si dispersoids. The peak at 290˚C is weak but well defined at the pre-strain of 3.5. This peak may correspond to precipitation of Si, but this cannot be concluded without support of dedicated TEM investigations. For the same strain a more broad peak occurs in the temperature range of interest from 200-230˚C. However, at the two severe strains of 5 and 7.4 a strong exothermic peak appeared in the range 250-300˚C. This peak overlaps with the two lowermost peaks observed at the lower strain and could be due to Si precipitation occurring at lower temperatures due to enhanced diffusion in the severely deformed specimens. Since the DSC scans were carried out at a heating rate of 10°C/min in helium atmosphere, the scans indicate that some kind of precipitation or clustering may be occurring at time-temperature combinations relevant for HOA at 225˚C during 10 minutes.

Even though precipitates could not be observed in the TEM samples of AA3103 deformed to a strain of 4.2 and annealed at 225˚C for 10 minutes, their presence cannot be excluded as there is a chance of missing them in TEM observations due to a very small size. Since clustering of solute atoms is common during early stages of precipitation [18], it is a possibility that clusters might have formed during the first 10 minutes of annealing the deformed material and later transformed into the precipitates observed in Figure 10 subsequent to 4 hours annealing. Note from Figure 5 that HOA is still present after 4 hours, where the weak decrease of the HOA with increased annealing time is most likely due to static recovery.

During annealing at a temperature of 225°C, Si can quite easily diffuse in a short range by pipe diffusion along dislocations in a highly deformed material. Even though it follows from the discussion above that it is unlikely that Si is causing HOA as the only element in solid solution, these diffusion events might be towards other alloying elements, preferably Mn. Thus, diffusion of Si to the vicinity of Mn to form some type of Mn-Si clusters cannot be excluded as a part of an explanation of HOA in AA3103 alloys. The observation in Figure 15 that the HOA in AA3103-2 with the lowest amount of Si in solid solution is similar to the HOA in AA3103NH or AA3103-2 with more Si available, suggests that if Si is involved, only very small amounts of it in solid solution is required for HOA.

5. Summary and conclusion

Hardening on annealing in rolled AA3103 aluminium alloy is observed at annealing temperatures above 150˚C. The phenomenon requires a minimum strain and increases in magnitude with increasing rolling strains. The ultimate tensile strength is increased by the annealing. However, a permanent increase in yield stress requires a small amount of deformation subsequent to the annealing, for example by a few per cent cold rolling. For the cases of severe plastic deformation obtained by ARB the explanation of hardening on annealing by dislocation source limitation cannot be ignored, but the same explanation may not apply to the lowest strain of 1.7. Furthermore, the hardening on annealing in cold rolled AA3103 was not removed by a subsequent cold rolling deformation of 15%, strongly indicating that dislocation source limitation is not responsible for the phenomenon in this case. A broad range of annealing times and temperatures was examined in terms of tensile tests. Significant changes in the substructure could not be observed. The influence of varying levels of Mn and Si in solid solution was investigated by comparison of two alloys with various homogenization treatments. It is concluded that Mn plays a major role, since, at a rolling strain of 3.5, hardening on annealing was observed in AA3103 but not in an Al-Si alloy that had almost the same composition but without Mn. Moreover, in AA3103 the hardening on annealing had a comparable extent for the as-cast material with considerable amounts of Si and Mn in solution as for an “industrially” homogenized material and for a homogenization procedure designed to remove most of the Si from solid solution. Since the variations of Si in solution did not influence the magnitude of the hardening on annealing, it is likely that Si is not directly involved. Diffusion of Mn at 225°C during 10 minutes seems unlikely but dislocation core effects may play an important role in the diffusion of Si towards other elements. Thus, formation of solute clusters or precipitation of very small particles seems likely. The hardening on annealing behaviour in AA3103 has been reported and analysed but not fully explained here. More detailed investigations involving atom probe and atomistic simulations might provide insight and lead to an explanation of this behaviour.

References

1. Øyvind Ryen, Bjørn Holmedal, Oscar Nijs, Erik Nes, Emma Sjölander and Hans-Erik Ekström, *Metallurgical and Materials Transactions A* 2006, vol. 37, pp. 1999-2006.
2. Y. Saito, H. Utsunomiya, N. Tsuji and T. Sakai, *Acta Materialia* 1999, vol. 47, pp. 579-583.
3. X. Huang, N. Hansen and N. Tsuji, *Science* 2006, vol. 312, pp. 249-251.
4. Xiaoxu Huang, *Scripta Materialia* 2009, vol. 60, pp. 1078-1082.
5. Wei Zeng, Yao Shen, Ning Zhang, Xiaoxu Huang, Jeff Wang, Guoyi Tang and Aidang Shan, *Scripta Materialia* 2012, vol. 66, pp. 147-150.
6. Naoya Kamikawa, Xiaoxu Huang, Nobuhiro Tsuji and Niels Hansen, *Acta Materialia* 2009, vol. 57, pp. 4198-4208.
7. N. H. Lee, P. W. Kao, T. Y. Tseng and J. R. Su, *Materials Science and Engineering: A* 2012, vol. 535, pp. 297-305.
8. R Shoji and C Fujikura, *Key Engineering Materials* 1990, vol. 44 & 45, pp. 163 - 180.
9. Q. Zhao, B. Holmedal, Y. Li. *Philosophical Magazine* 2013, http://dx.doi.org/10.1080/14786435.2013.794315
10. X. Huang, N. Kamikawa and N. Hansen, *Materials Science and Engineering A* 2008, vol. 493, pp. 184-189.
11. Daisuke Terada, Hironobu Houda and Nobuhiro Tsuji, *Journal of Materials Science* 2008, vol. 43, pp. 7331-7337.
12. W.C. Liu and B. Radhakrishnan, *Materials Letters* 2010, vol. 64, pp. 1829-1832.
13. J. Morris and W. Liu, *JOM Journal of the Minerals, Metals and Materials Society* 2005, vol. 57, pp. 44-47.
14. Stian Tangen, Knut Sjølstad, Erik Nes, Trond Furu and Knut Marthinsen, *Materials Science Forum* 2002, vol. 396-402, pp. 469-474.
15. Y. J. Li and L. Arnberg, *Acta Materialia* 2003, vol. 51, pp. 3415-3428.
16. Y. Du, Y. A. Chang, B. Huang, W. Gong, Z. Jin, H. Xu, Z. Yuan, Y. Liu, Y. He and F. Y. Xie, *Materials Science and Engineering A* 2003, vol. 363, pp. 140-151.
17. B. Forbord, W. Lefebvre, F. Danoix, H. Hallem and K. Marthinsen, *Scripta Materialia* 2004, vol. 51, pp. 333-337.
18. G. A. Edwards, K. Stiller, G. L. Dunlop and M. J. Couper, *Acta Materialia* 1998, vol. 46, pp. 3893-3904.
19. M. A. Kenawy, G. Graiss, G. Saad and A. Fawzy, *Journal of Physics D: Applied Physics* 1987, vol. 20, p. 125.
20. E. Clouet and A. Barbu, *Acta Materialia* 2007, vol. 55, pp. 391-400.

ACKNOWLEDGEMENTS

The present study was financed by the Norwegian Research Council under the Improvement project of the Strategic University Program (192450/I30).